Supplementary Note 1

Because we confirmed good material balance in the presence of an internal standard (98.5–99.5%), conversion, yield, and selectivity were defined as follows to improve accuracy of the values especially at a low conversion:

$$\text{Conversion}_{CH_4}\ (\%) = \frac{n_{CO} + n_{CO_2}}{n_{CH_4} + n_{CO} + n_{CO_2}} \times 100\% \quad (1)$$

$$\text{Yield}_{CO}\ (\%) = \frac{n_{CO}}{n_{CH_4} + n_{CO} + n_{CO_2}} \times 100\% \quad (2)$$

$$\text{Yield}_{CO_2}\ (\%) = \frac{n_{CO_2}}{n_{CH_4} + n_{CO} + n_{CO_2}} \times 100\% \quad (3)$$

$$\text{Selectivity}_{CO}\ (\%) = \frac{n_{CO}}{n_{CO} + n_{CO_2}} \times 100\% \quad (4)$$

$$H_2/CO = \frac{n_{H_2}}{n_{CO}} \quad (5)$$

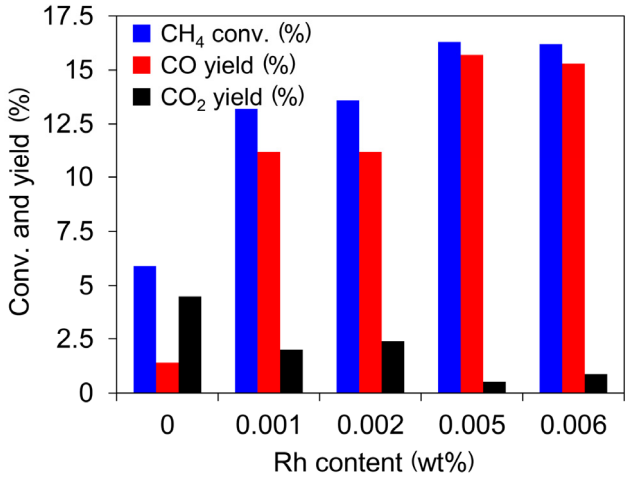

Supplementary Figure 1 Effect of loading amount of Rh on POM at 600 °C, SV = 12,000 mL h^{-1} g^{-1}, and $CH_4/O_2/He$ = 50/4/46.

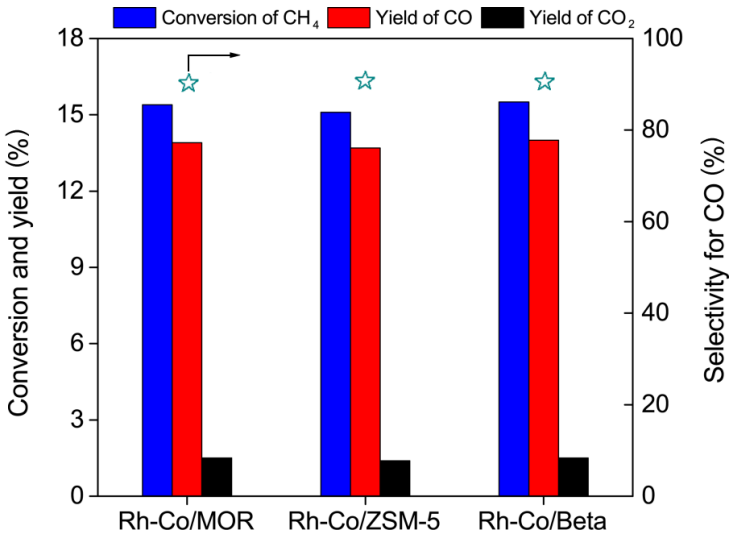

Supplementary Figure 2 Screening of zeolite supports in POM at 600 °C, SV = 60,000 mL h^{-1} g^{-1}, and $CH_4/O_2/He$ = 50/4/46. Star symbols: selectivity for CO.

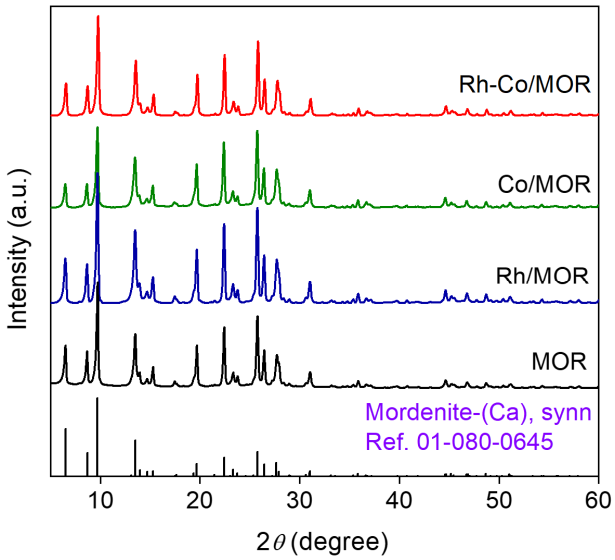

Supplementary Figure 3 XRD patterns of different samples.

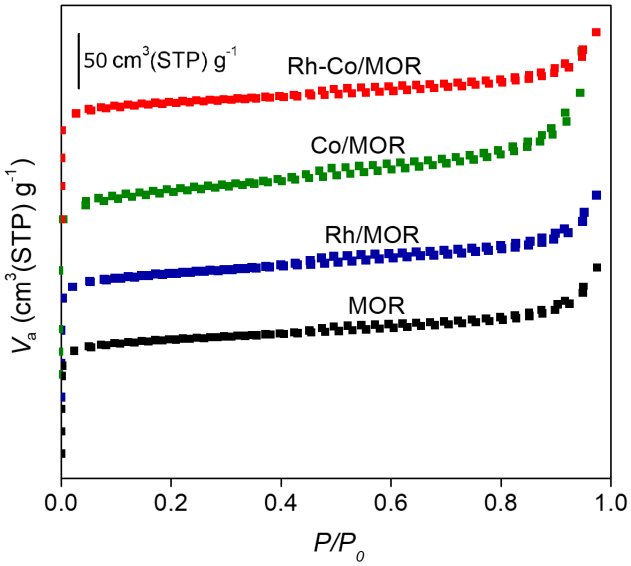

Supplementary Figure 4 N_2 adsorption-desorption isotherms at −196 °C for different samples.

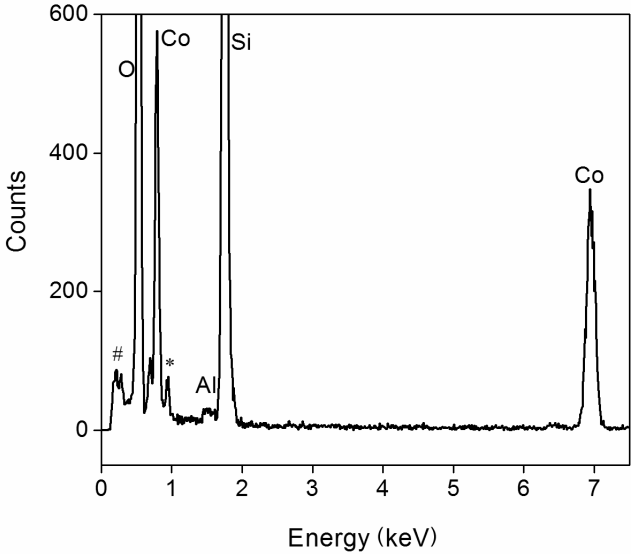

Supplementary Figure 5 EDX spectrum of Rh-Co/MOR at bright dots. #C and *Cu come from the holey carbon-supported copper grid.

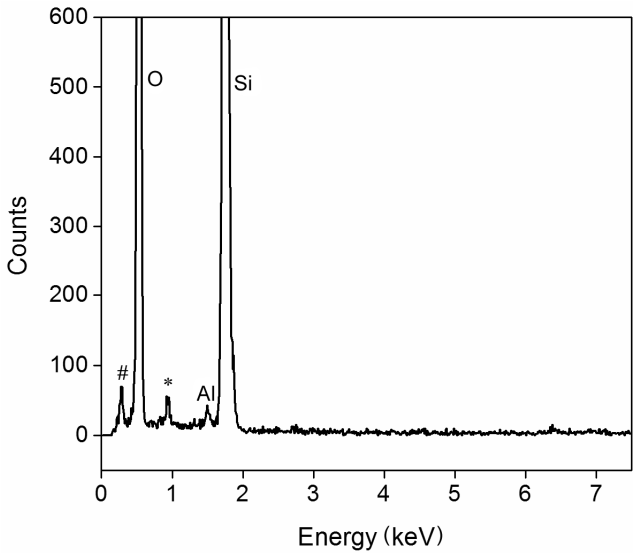

Supplementary Figure 6 EDX spectrum of Rh-Co/MOR at dark area. #C and *Cu come from the holey carbon-supported copper grid.

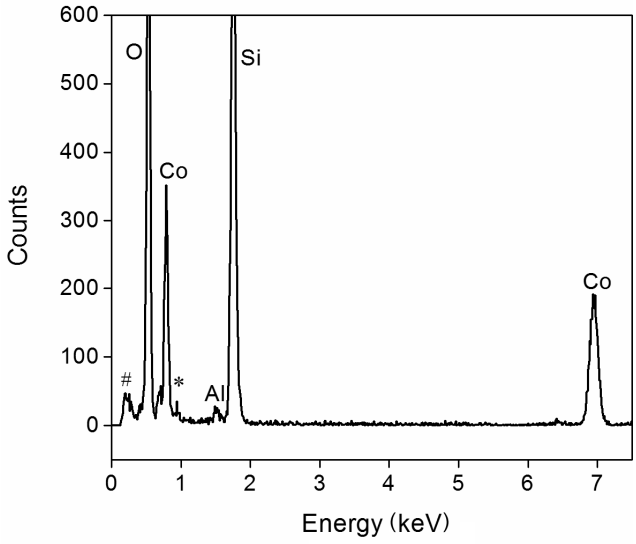

Supplementary Figure 7 EDX spectrum of Co/MOR at bright dots. #C and *Cu come from the holey carbon-supported copper grid.

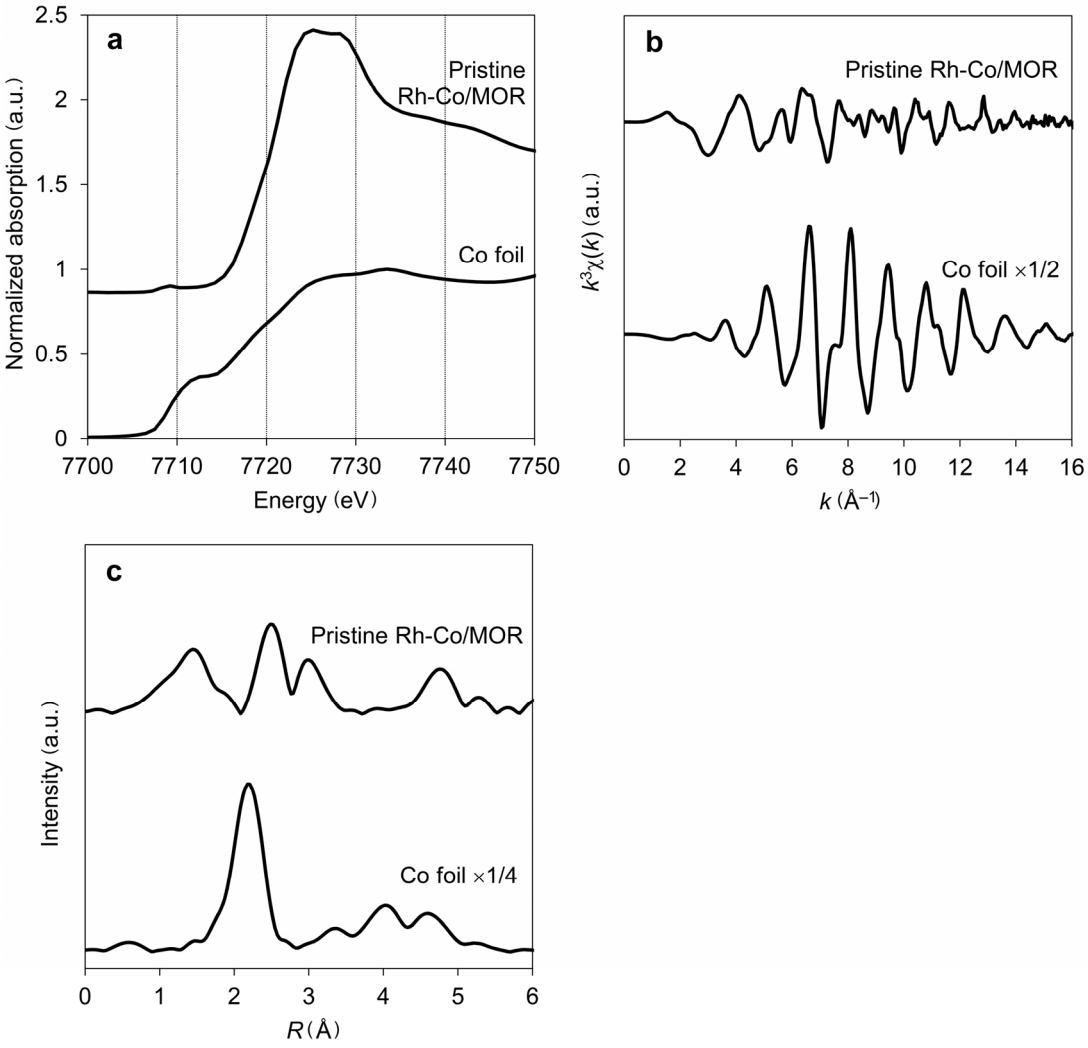

Supplementary Figure 8 Co K-edge XAFS analysis. XANES spectra (**a**), EXAFS oscillations (**b**), and Fourier transforms of the EXAFS data (**c**). Data was collected in transmission mode with a harmonic rejection mirror. In XANES, pristine Rh-Co/MOR provided peak tops at 7725 and 7728 eV, the range for Co^{2+}, whereas Co^{3+} gives a peak top at higher than 7730 eV.[1,2]

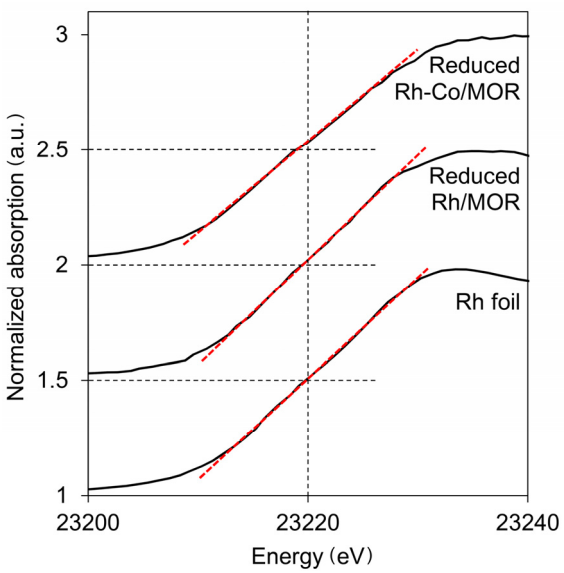

Supplementary Figure 9 Enlarged image of Rh K-edge XANES spectra. Red lines are tangents to the absorption edges. Horizontal dashed lines show normalized absorption of 0.5 for the respective spectra.

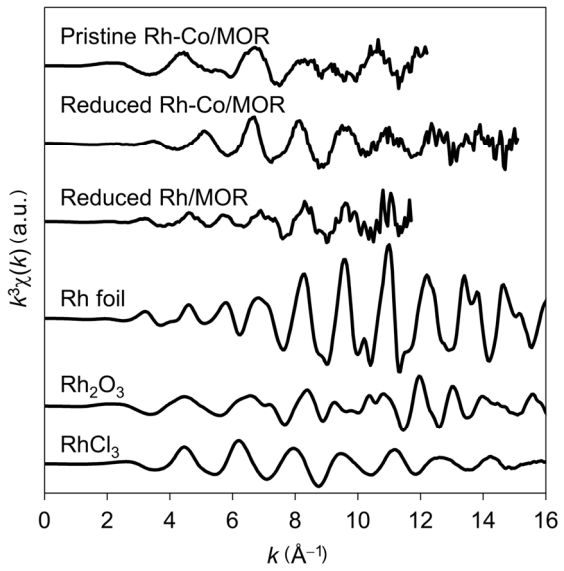

Supplementary Figure 10 Rh K-edge k^3-weighted EXAFS oscillations.

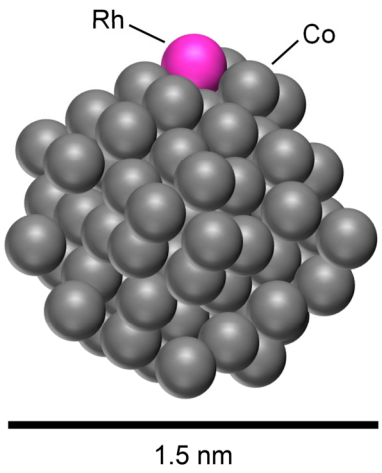

Supplementary Figure 11 Model structure of a Rh–Co particle on reduced Rh-Co/MOR.

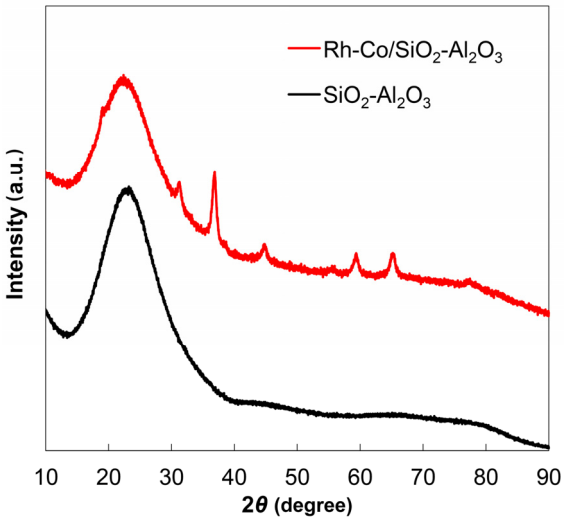

Supplementary Figure 12 XRD patterns of Rh-Co/SiO_2-Al_2O_3 and SiO_2-Al_2O_3. Crystallite size of Co_3O_4 is 12 nm.

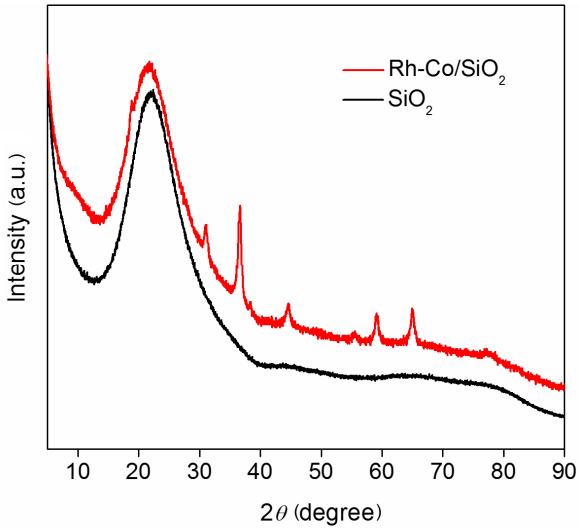

Supplementary Figure 13 XRD patterns of Rh-Co/SiO_2 and SiO_2. Crystallite size of Co_3O_4 is 13 nm.

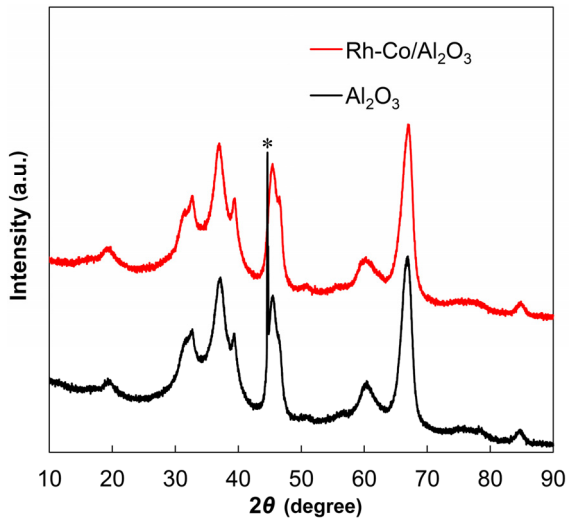

Supplementary Figure 14 XRD patterns of Rh-Co/Al_2O_3 and Al_2O_3. *Ghost peak.

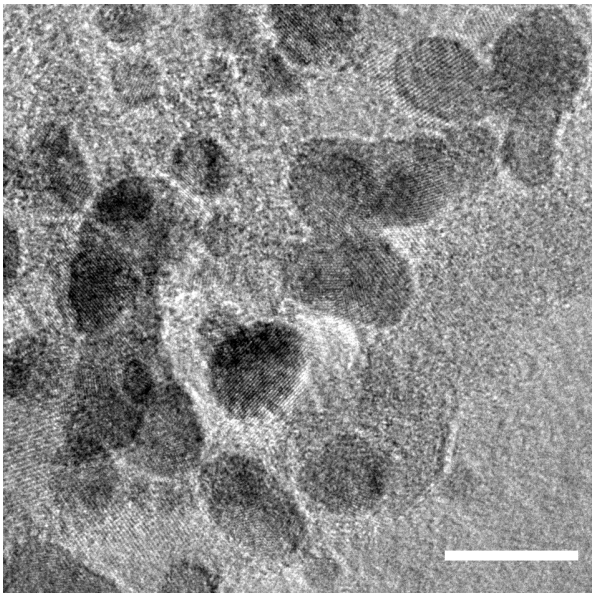

Supplementary Figure 15 TEM image of Rh-Co/SiO_2. Scale bar: 10 nm. Lattice fringe of Co_3O_4 can be seen.

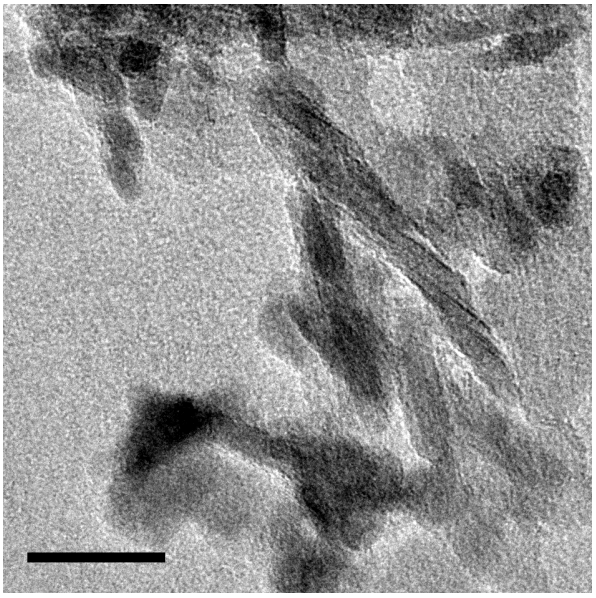

Supplementary Figure 16 TEM image of Rh-Co/Al_2O_3. Scale bar: 20 nm. Clear Rh-Co particles were not observed.

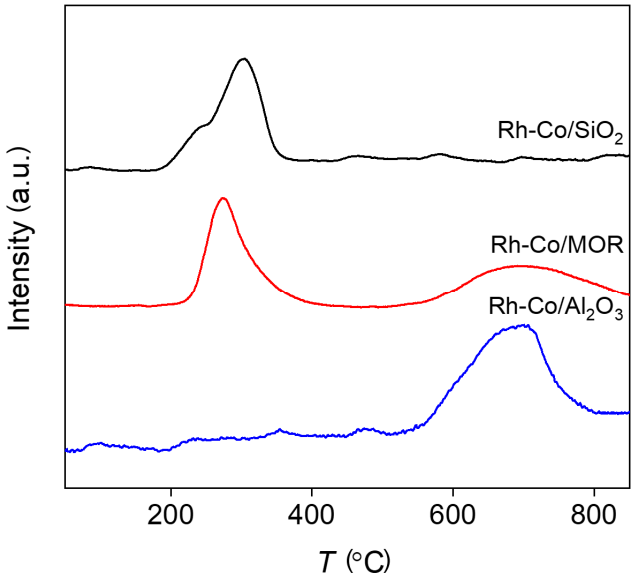

Supplementary Figure 17 TPR profiles of Rh-Co bimetallic catalysts. The profiles were normalized to the same peak height since the measurement instruments and sensitivities were different.

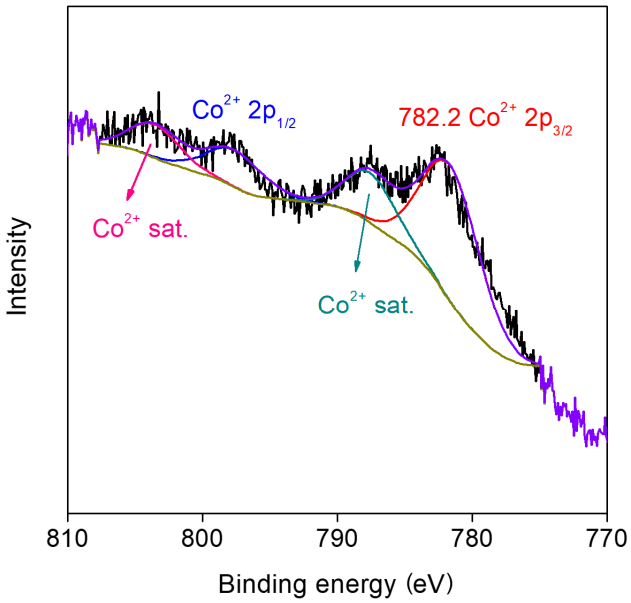

Supplementary Figure 18 Co 2p XPS for spent Co/MOR after methane oxidation at 600 °C. Black line: raw experimental data, coloured lines: curve fitting data. sat.: satellite peak.

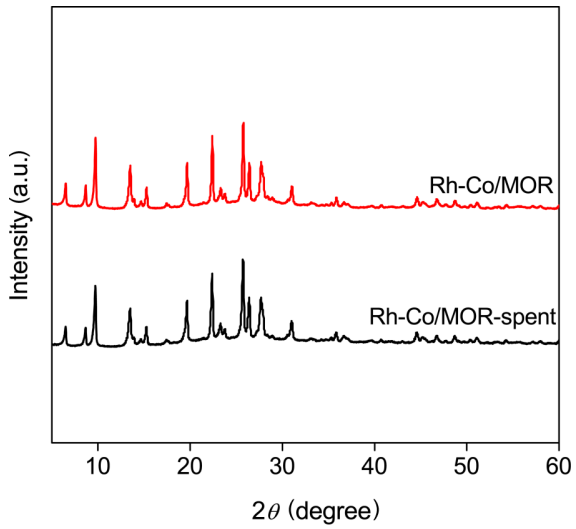

Supplementary Figure 19 XRD patterns of fresh Rh-Co/MOR and that after POM. The POM was performed at 650 °C, $CH_4/O_2/N_2$ = 3.33/1.67/95, SV = 1,200,000 mL h^{-1} g^{-1} for 50 h. Measurement conditions are different from those in Supplementary Figure 3, due to the smaller amount of catalyst.

Supplementary Table 1 Properties of samples

Sample	BET surface area /m^2 g^{-1}	Micropore volume[a] /cm^3 g^{-1}
MOR	520	0.19
Rh-Co/MOR	490	0.18
Rh/MOR	500	0.19
Co/MOR	500	0.18

[a] *t*-Plot method.

Supplementary Table 2 Curve fitting analysis of Co K-edge EXAFS spectra using FEFF table

Sample	Shell	CN	*R* /Å	σ^2 /Å^2	R factor /%
Pristine Rh-Co/MOR	Co–O	5.1	1.97	0.017	3.6
	$Co–Co_{1st}$	2.0	2.83	0.0056	
	$Co–Co_{2nd}$	1.5	3.38	0.0030	
	$Co–Co_{3rd}$	4.7	5.04	0.0031	
Co foil	Co–Co	9.5	2.49	0.0045	1.1

Supplementary Table 3 Amount of coke deposition on catalyst after methane oxidation at 600 °C

Catalyst	Reaction time /h	Coke /wt%
Rh-Co/MOR	2	0.02
Rh-Co/MOR	18	0.10
Co/MOR	2	0.15
$Rh-Co/SiO_2$	2	2.7
$Rh-Co/Al_2O_3$	18	0.12

Supplementary references

1 Wang, Y., Zhang, C., Liu, F. & He, H. Well-dispersed palladium supported on ordered mesoporous Co_3O_4 for catalytic oxidation of *o*-xylene. *Appl. Catal. B: Environ.* **142-143**, 72-79 (2013).

2 Junheng, H., Qinghua, L., Tao, Y., Zhiyun, P. & Shiqiang, W. XAFS study on structure-activity correlations of α-$Co(OH)_2$ nanosheets water oxidation catalysts. *J. Phys.: Conf. Ser.* **712**, 012128 (2016).